Supramolecular Chemistry with Macromolecules: New Self-Assembly based Main Chain Polypseudorotaxanes and Their Properties

Caiguo Gong, Peter B. Balanda, and Harry W. Gibson*

Department of Chemistry, Virginia Polytechnic Institute and State University, Blacksburg, Virginia 24061

Received December 23, 1997; Revised Manuscript Received June 10, 1998

ABSTRACT: A new class of main chain polypseudorotaxanes, **8**, was prepared by self-assembly of a poly(ester crown ether), poly[bis(5-methylene-1,3-phenylene)-32-crown-10 sebacate] (**5**), and *N*,*N*′-bis(*β*-hydroxyethyl)-4,4′-bipyridinium bis(hexafluorophosphate) (**6**). The equilibrium constant ($K = 58.0$ M^{-1} at 21.8 °C), ΔH (−26.5 kJ/mol) and ΔS (−56.4 J/mol deg)(all averages from several iterative methods) for the formation of **8** were measured by proton NMR spectroscopy. Compared to those ($K = 247$ M^{-1} at 21.8 °C, $\Delta H = -44.7$ kJ/mol, $\Delta S = -106$ J/mol deg) for the model system, bis(5-acetoxymethyl-*m*-phenylene)-32-crown-10 (**4**) and **6**, the enthalpy term is less favorable for the polymeric system, while the entropy term is less unfavorable. The measured values enabled us to design polypseudorotaxanes with targeted degrees of threading (*m*/*n*, the fraction of the cyclic moieties threaded with linear species). The solubility of polypseudorotaxane **8** was different from both starting materials **5** and **6**, and depended on the *m*/*n* value. Polypseudorotaxanes **8** with higher *m*/*n* had higher viscosities because of increased hydrodynamic volume in solution and were more rigid as manifested by higher glass transition temperatures (T_g) in the solid state. Dethreading (decomplexation) took place above T_g in the solid state, causing loss of color (orange), a process potentially useful for temperature sensors.

Introduction

Physically linked molecular structures, e.g., rotaxanes and catenanes,[1] have opened a new window for polymer scientists in terms of polymer topology. As molecular composites, polyrotaxanes have indeed become an active research topic.[1−9] According to the location of the rotaxane unit, polyrotaxanes can be divided into main chain systems, in which the rotaxane moiety is a main chain unit, and side chain systems, in which the rotaxane unit is a pendant group or side chain moiety. In the main chain category, both polypseudorotaxanes (Scheme 1: **1**) and true polyrotaxanes (**1**′) are possible using cyclic components of low molar mass; similarly, main chain polypseudorotaxanes (**2**) and true polyrotaxanes (**2**′) are in principle available from polymers containing cyclic repeat units.[1a,d,f] To our knowledge, however, only main chain systems of types **1** and **1**′ have been constructed; up until now no systems of types **2** or **2**′ have appeared in the literature.

In addition to the chemical compositions of the backbone and the cyclic, the properties of polyrotaxanes mainly depend on the extent of threading (*m*/*n*, the fraction of the cyclic moieties threaded with linear species).[1] To achieve high *m*/*n* values, a strong attractive force between the cyclic and linear species, a driving force for threading, is indeed necessary.[1] Two types of driving forces have often been used for the synthesis of polyrotaxanes: inclusion complexation for cyclodextrin-based systems[1−3] and hydrogen bonding for many crown ether-based systems.[1,4−6] It has been well demonstrated by Stoddart's group that self-assembly accomplished by *π*-stacking, hydrogen bonding, and dipolar−diploar interactions between electron-rich arylene-based crown ethers and electron-poor 4,4′-bipyridinium salts can play a very powerful and important role in the field of *supra*molecular chemistry.[1,10] A wide variety of pseudorotaxanes, rotaxanes, and catenanes based on these systems have been reported. Their formation is characterized by the instantaneous development of red or orange coloration due to charge transfer interactions of the donor and acceptor moieties, by upfield shifts of the time-averaged signals for the aromatic protons in the NMR spectra and finally by their single-crystal X-ray structures.[1,10,11] However, only a few polypseudorotaxanes have been prepared based on such driving forces.[7] Polypseudorotaxanes of type **1** were prepared by threading a bisparaquat cyclophane onto linear polymers bearing electron rich moieties in solution; no physical properties were reported.[7e−7 g] Polypseudorotaxanes of type **1** with backbones containing paraquat moieties were also prepared by threading with crown ethers.[7a−7c] Interactions of pendant cyclic host units of polymers with *N*,*N*′-dialkyl-4,4′-bipyridinium species provided the basis of novel sensors.[7d] Metal templating of phenanthroline-containing crown ethers with linear phenanthroline- or 2,2′-bipyridine-containing ligands has also been employed in the construction of types **1** and **1**′ systems.[9]

Here, we report an approach for the preparation of new main chain polypseudorotaxanes of type **2** by self-assembly of a preformed poly(ester crown ether) with a low molar mass *N*,*N*′-dialkyl-4,4′-bipyridinium (paraquat)

Scheme 1

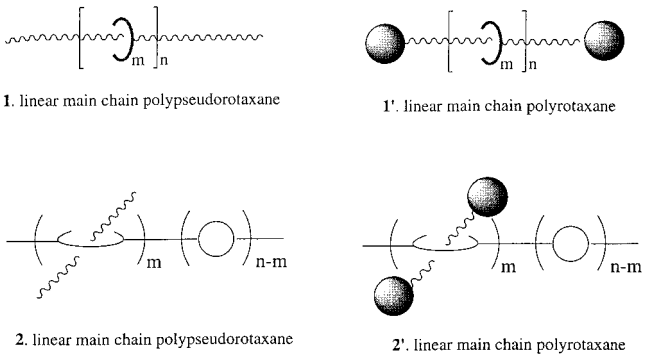

1. linear main chain polypseudorotaxane

1'. linear main chain polyrotaxane

2. linear main chain polypseudorotaxane

2'. linear main chain polyrotaxane

S0024-9297(97)01857-3 CCC: $15.00
Published on Web 07/17/1998

Scheme 2

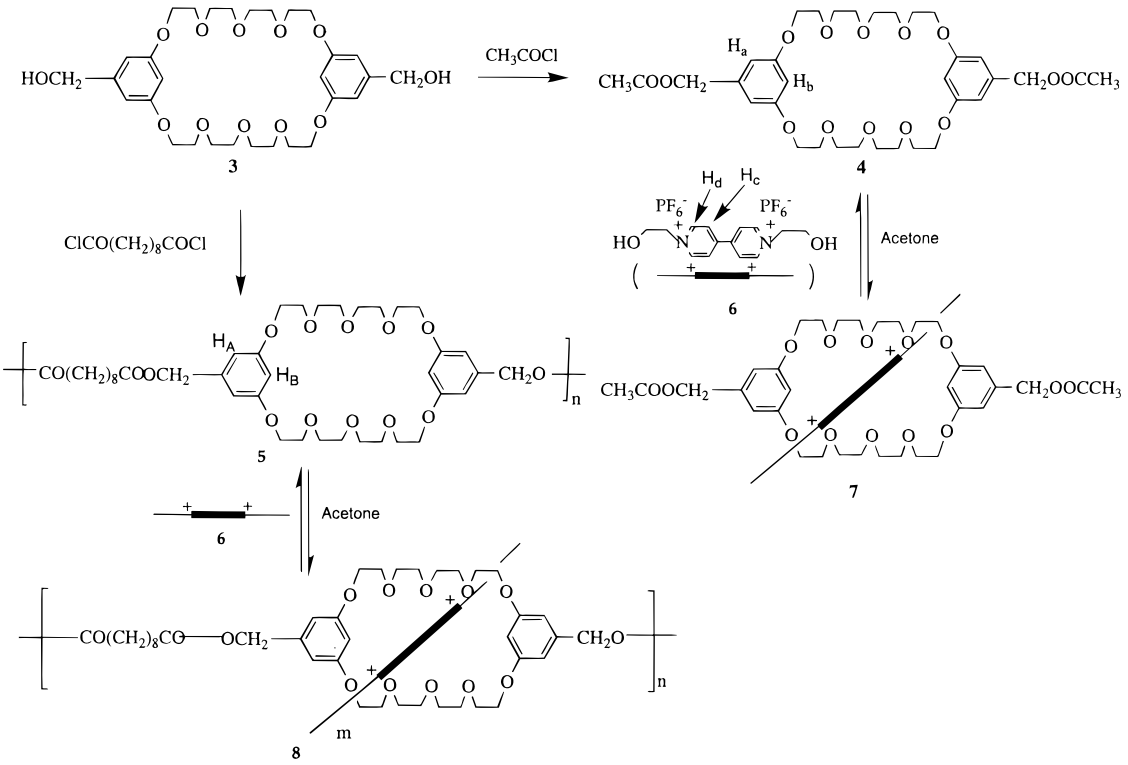

derivative. Some properties of these polypseudorotaxanes, both in solution and solid states, were also studied.

Results and Discussion

I. Synthesis of Precursors. To prepare the desired polypseudorotaxanes of type **2** by self-assembly, both *N*,*N*′-dialkyl-4,4′-bipyridinium salts and polymeric crown ethers are necessary. Bis(5-hydroxymethyl-1,3-phenylene)-32-crown-10 (**3**) is a good macrocycle for this purpose because its ring size and chemical composition ensure its ability to complex with paraquat[1,10] and the reactive hydroxyl groups are useful for polymerization with other monomers.[6b,6c]

Macrocycle **3** (Scheme 2) was synthesized by a reported procedure.[12] It was then quantitatively converted into bis(5-acetoxymethyl-1,3-phenylene)-32-crown-10 (**4**) by reaction with acetyl chloride in THF.[12] The solution polycondensation of **3** with sebacoyl chloride afforded poly[bis(5-methylene-1,3-phenylene)-32-crown-10 sebacate] (**5**) (Scheme 2). We have shown that self-association of hydroxymethyl or carboxy derivatives of this parent crown ether (via H-bonding of the −OH groups with the ether oxygen atoms) leads to branched or cross-linked products, i.e, self-threaded polyrotaxanes, upon polycondensation with complimentary functionalities in the absence of strongly H-bonding solvents.[6] We have also shown that use of DMSO, a strong H-bond acceptor, as solvent completely suppresses this self-threading process.[6c] Thus, in the present work, to obtain a linear polymer, DMSO was used as a cosolvent in the polymerization.

N,*N*′-Bis(*β*-hydroxyethyl)-4,4′-bipyridinium bis(hexafluorophosphate) (**6**) was prepared from 4,4′-bipyridine and *β*-hydroxyethyl iodide, followed by counterion exchange.[11] The purpose of the ion exchange is to increase the solubility of the paraquat salt in organic solvents.[10]

II. Complexation. (a) Model study: [2]Pseudorotaxane 7. Stoddart's group has extensively studied the complexation of bisarylene-based crown ethers with paraquats.[1,10] More specifically, they found that bis(*m*-phenylene)-32-crown-10 complexes with *N*,*N*′-dimethyl-4,4′-bipyridinium bis(hexafluorophosphate) and reported an equilibrium constant (K = 760 M^{-1} in acetone at ambient temperature by UV spectroscopy).[10a] However, to our knowledge no enthalpy (ΔH) or entropy changes (ΔS) have been reported for pseudorotaxane formation from crown ethers and paraquat derivatives. We consider these thermodynamic parameters to be very important in terms of quantitatively understanding the complexation process. Here, we demonstrate the successful utilization of proton NMR spectroscopy for this purpose. For comparison with the polyester **5**/**6** system, diester **4** and paraquat **6** were used in a model complexation study.

As soon as host **4** and guest **6** were mixed, the solution turned orange, indicating the rapid formation of [2]-pseudorotaxane **7**.[1,10,11] Relative to those of pure **4** (Figure 1a at 21.8 °C and Figure 1d at 38 °C, respectively), the time-averaged signals of protons H_a and H_b (see Scheme 2) of the cyclic were shifted upfield after complexation (parts b and c of Figure 1, respectively), indicating the formation of pseudorotaxane **7**.[1,7,10,11] Because the complexation is exothermic, increasing the temperature depressed the formation of **7**, as indicated by the fact that the time-averaged signals for protons H_a and H_b were shifted downfield toward the shifts of the signals for the uncomplexed species **4** (Figure 1c vs Figure 1b).

Only time-averaged signals were observed because the complexation was a rapid exchange process relative to the NMR time scale.[1,7,10,11] To calculate the equilibrium constant K, continuous titration was employed.[13] According to this method, the continuous addition of **6** into a solution containing a constant concentration of **4** gives the corresponding time-averaged signals, e.g., for proton H_a or H_b, and the Δ values; $\Delta = \delta_f - \delta$, where δ

Table 1. Chemical Shifts of Protons H_a and H_b of 4 upon Complexation with Different Amounts of 6 in Acetone at Different Temperatures[a]

	δ_a/δ_b[b] (ppm)				
$[\mathbf{6}]_o$ (mM)	21.8 °C	30.0 °C	38.0 °C	46.0 °C	54.0 °C
0	6.523/6.452	6.525/6.458	6.527/6.464	6.529/6.469	6.531/6.475
11.63	6.177/6.149	6.239/6.191	6.312/6.246	6.370/6.296	6.417/6.340
23.25	6.084/6.069	6.154/6.106	6.230/6.162	6.292/6.214	6.353/6.269
27.44	6.073/6.059	6.144/6.097	6.219/6.150	6.283/6.200	6.343/6.253
39.23	6.040/6.031	6.095/6.056	6.162/6.096	6.232/6.148	6.302/6.209
44.18	6.034/6.025	6.092/6.049	6.156/6.087	6.221/6.134	6.286/6.189
65.16	6.018/6.011	6.073/6.030	6.133/6.063	6.191/6.104	6.261/6.159
122.4	5.990/5.990	6.033/5.993	6.082/6.013	6.136/6.042	6.194/6.081

[a] $[\mathbf{4}]_o$ constant at 7.350 mM; temp, ±0.1 °C. [b] δ_a/δ_b: the chemical shifts of the protons H_a and H_b, respectively; ±0.001 ppm.

Table 2. Chemical Shift Changes of Protons H_a and H_b of 4 (7.350 mM Initially) upon Complexation with Different Amounts of 6 in Acetone at Different Temperatures

	Δ_a/Δ_b[a] (ppm)				
$[\mathbf{6}]_o$ (mM)	21.8 °C	30.0 °C	38.0 °C	46.0 °C	54.0 °C
0	0.000/0.000	0.000/0.000	0.000/0.000	0.000/0.000	0.000/0.000
11.63	0.346/0.303	0.286/0.267	0.215/0.218	0.159/0.173	0.114/0.135
23.25	0.439/0.383	0.371/0.352	0.297/0.302	0.237/0.255	0.178/0.206
27.44	0.450/0.393	0.381/0.361	0.308/0.314	0.246/0.269	0.188/0.222
39.23	0.483/0.421	0.430/0.402	0.365/0.368	0.297/0.321	0.229/0.266
44.18	0.489/0.427	0.433/0.409	0.371/0.377	0.308/0.335	0.245/0.286
65.16	0.505/0.441	0.452/0.428	0.394/0.401	0.338/0.365	0.270/0.316
122.4	0.533/0.462	0.492/0.465	0.445/0.451	0.393/0.427	0.337/0.394

[a] Δ_a/Δ_b: the chemical shifts changes of the protons H_a and H_b compared to those of pure **4** at the same temperature, respectively; ±0.002 ppm.

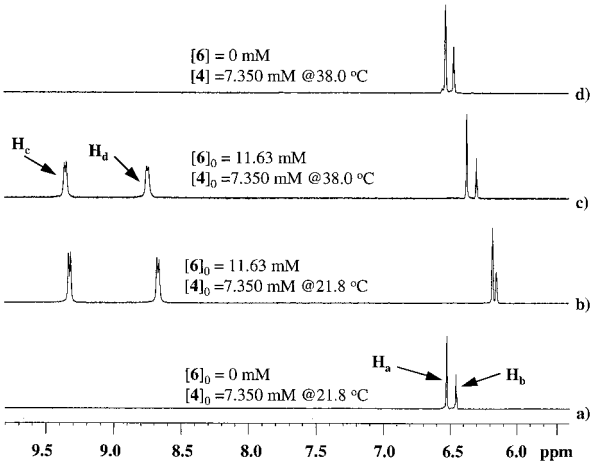

Figure 1. Expanded aromatic regions of the 400 MHz proton NMR spectra for (a and d) **4** and for (b and c) solutions of **4** and **6** in acetone-d_6.

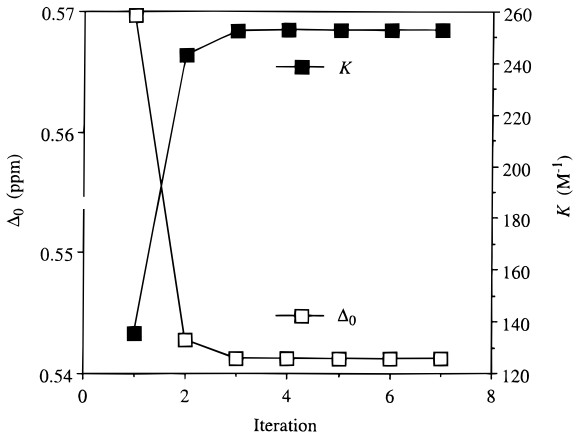

Figure 2. Dependence of K and Δ_o on the iteration number in the Benesi−Hildebrand treatment of data for proton H_a for the formation of [2]pseudorotaxane **7** with $[\mathbf{4}]_o = 7.350$ mM at 21.8 °C in acetone.

is the time-averaged chemical shift of the partially complexed solution and δ_f is the chemical shift of the free or uncomplexed form, i.e., pure **4**. To determine K, ΔH and ΔS, the chemical shifts of protons H_a and H_b were measured by varying both the total initial concentration of **6**, $[\mathbf{6}]_o$, and temperature with the total initial concentration of **4**, $[\mathbf{4}]_o$, fixed at 7.350 mM in acetone (Table 1). The corresponding Δ values were then calculated (Table 2).

There are two unknowns to be evaluated: the equilibrium constant K and Δ_o, which is the chemical shift difference between free and 100% complexed forms, i.e., $\Delta_o = \delta_f - \delta_c$; δ_c is the chemical shift of the totally complexed form, e.g., proton H_a or H_b of **7**. A number of methods have been developed to estimate these two parameters.[13] We have applied iterative techniques to linear methods initially reported by (1) Benesi and Hildebrand[14] and (2) Scatchard[15] and have compared these results to those from methods reported by (3) Cresswell and Allred[16] and (4) Rose and Drago.[17]

In the Benesi−Hildebrand method, inverse values of Δ are plotted vs $1/[\mathbf{6}]$ in the form $1/\Delta = 1/(\Delta_o K[\mathbf{6}]) + 1/\Delta_o$; traditionally $[\mathbf{6}]_o$, the total initial concentration of **6**, is used as an estimate of the concentration of uncomplexed **6**, $[\mathbf{6}]$. The intercepts of these plots give estimates of Δ_o and from the slope K can be calculated. We used this Δ_o value to produce a refined estimate of $[\mathbf{6}]$, since $[\mathbf{6}] = [\mathbf{6}]_o - (\Delta/\Delta_o)[\mathbf{4}]_o$. Replotting the data using the new estimate of $[\mathbf{6}]$ provided improved estimates of Δ_o and K. The process was repeated until constancy of these two parameters was achieved. In the present case seven iterations were done, although the values became constant (<0.1% variation) after three iterations (Figure 2). The first and seventh generation plots are compared in Figure 3. The results are given in Table 3.

In the Scatchard method $\Delta/[\mathbf{6}]$ is plotted vs Δ in the form $\Delta/[\mathbf{6}] = -K\Delta + K\Delta_o$. Again, traditionally $[\mathbf{6}]_o$ is

Table 3. Association Constants for the Complexation of 4 at Different Temperatures with Variable Amounts of 6 in Acetone-d_6 As Determined by Iterative Benesi−Hildebrand Plotting Techniques[a] (See Figure 2)

					Δ_0 (ppm)		
T (°C)	proton	slope (mM·ppm)	intercept (ppm^{-1})	R^2	entered	calcd	K^b (M^{-1})
21.8	H_a	7.3083	1.84785	0.996	0.54117	0.54117	253 ± 18
21.8	H_b	8.2003	2.12497	0.997	0.47060	0.47060	259 ± 17
30.0	H_a	11.2894	2.01205	0.986	0.49700	0.49700	178 ± 26
30.0	H_b	12.4197	2.11730	0.991	0.47230	0.47230	170 ± 19
38.0	H_a	20.9063	2.16747	0.988	0.46137	0.46137	104 ± 15
38.0	H_b	20.6347	2.13355	0.990	0.46870	0.46870	103 ± 13
46.0	H_a	35.5744	2.34737	0.994	0.42601	0.42601	66.0 ± 7.2
46.0	H_b	32.5665	2.17148	0.995	0.46051	0.46051	66.7 ± 6.7
54.0	H_a	58.2528	2.65797	0.996	0.37623	0.37623	45.6 ± 5.2
54.0	H_b	48.4801	2.31018	0.995	0.43287	0.43287	47.6 ± 5.8

[a] Δ_0 and K values were obtained from the seventh generation Benesi−Hildebrand plot. [b] Error estimates are based on statistically determined confidence limits of the intercept and slope at the 95% probability level propagated according to

$$\Delta K = K\sqrt{\left(\frac{\Delta\text{intercept}}{\text{intercept}}\right)^2 + \left(\frac{\Delta\text{slope}}{\text{slope}}\right)^2}$$

Table 4. Association Constants for the Complexation of 4 at Different Temperatures with Variable Amounts of 6 in Acetone-d_6 As Determined by Iterative Scatchard Plotting Techniques[a]

					Δ_0 (ppm)		
T (°C)	proton	slope (mM^{-1})	intercept (ppm·mM^{-1})	R^2	entered	calcd	K^b (M^{-1})
21.8	H_a	−0.24654	0.133907	0.992	0.543138	0.543138	246 ± 25
21.8	H_b	−0.25357	0.119697	0.994	0.472039	0.472039	254 ± 22
30.0	H_a	−0.16505	0.083225	0.971	0.504233	0.504233	165 ± 33
30.0	H_b	−0.16067	0.076753	0.981	0.477704	0.477704	161 ± 26
38.0	H_a	−0.09449	0.044689	0.97	0.472978	0.472978	94 ± 19
38.0	H_b	−0.09499	0.045543	0.975	0.479437	0.479437	95 ± 17
46.0	H_a	−0.06102	0.026705	0.981	0.437671	0.437671	61.0 ± 9.7
46.0	H_b	−0.06136	0.029076	0.982	0.473819	0.473819	61.4 ± 9.5
54.0	H_a	−0.04109	0.016153	0.975	0.393112	0.393112	41.1 ± 7.6
54.0	H_b	−0.04199	0.019149	0.972	0.456061	0.456061	42.0 ± 8.1

[a] Δ_0 and K values were obtained from the seventh generation Scatchard plot. [b] Error estimates are based on statistically determined confidence limits of the slope at the 95% probability level.

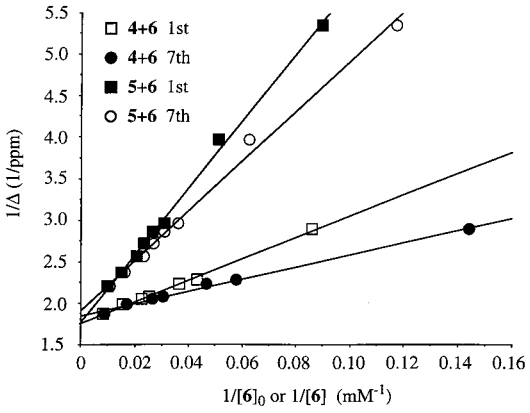

Figure 3. First (□ and ■) and seventh (○ and ●) generation Benesi−Hildebrand plots for the formation of [2]pseudorotaxane **7** with $[\mathbf{4}]_o = 7.350$ mM based on data for proton H_a and for the formation of polypseudorotaxane **8** with $[\mathbf{5}]_o = 7.340$ mM based on data for proton H_A, at 21.8 °C in acetone.

used to approximate [**6**] and thus estimate K and Δ_o. We calculated improved estimates from $[\mathbf{6}] = [\mathbf{6}]_o - (\Delta/\Delta_o)[\mathbf{4}]_o$ using the Δ_o values derived from the slopes and intercepts. Again, three iterations produced constant values of Δ_o and K; seven iterations were carried out to produce the results shown in Table 4.

The Cresswell−Allred treatment involves plotting observed δ values vs [**7**]/[**6**] in the form $\delta = ([\mathbf{7}]/[\mathbf{6}])\Delta_o + \delta_f$. Values of [**7**]/[**6**] are calculated from the quadratic solution of the equilibrium constant expression with the known initial concentrations by assuming an initial value for K. The assumed value of K was adjusted until the intercept converged on the measured experimental value of δ_f, at which time a marked improvement in the linearity of the data was also observed via the correlation coefficient, R. Results are given in Table 5.

Table 5. Association Constants for the Complexation of 4 at Different Temperatures with Variable Amounts of 6 in Acetone-d_6 As Determined by Iterative Creswell−Allred Plotting Techniques

T (°C)	proton	|slope| = Δ_0 (ppm)	intercept (ppm)	R^2	$\delta_{\text{intercept}}/\delta_{\text{free}}$[a]	K^b (M^{-1})
21.8	H_a	0.5437	6.523	0.995	1.00000001	244 ± 55
21.8	H_b	0.4726	6.452	0.996	1.00000009	251 ± 38
30.0	H_a	0.5055	6.525	0.984	1.00000002	162 ± 45
30.0	H_b	0.4791	6.458	0.989	1.00000005	158 ± 38
38.0	H_a	0.4757	6.527	0.988	0.99999994	91.9 ± 11
38.0	H_b	0.4825	6.464	0.990	1.00000000	92.2 ± 10
46.0	H_a	0.4416	6.529	0.994	1.00000001	59.4 ± 3.9
46.0	H_b	0.4785	6.469	0.994	0.99999999	59.3 ± 4.3
54.0	H_a	0.3986	6.531	0.992	1.00000001	39.5 ± 2.9
54.0	H_b	0.4641	6.475	0.991	1.00000000	39.9 ± 3.1

[a] The number of digits displayed is not meant to suggest degree of significance, but rather to illustrate the degree of convergence used to obtain K. [b] Δ_0 determined from the slope was used to calculate K at each temperature according to the expression

$$K = \frac{1}{\left(\frac{\Delta_0}{\Delta} - 1\right)[S_0] - \left(1 - \frac{\Delta}{\Delta_0}\right)[R_0]}$$

The confidence interval about the mean at the 95% probability level is used here to express the uncertainty in K.

The Rose−Drago method involves assumption of various Δ_o values and plots of K^{-1} vs Δ_o for each data point at a given temperature; K is derived according to

Table 6. Association Constants for the Complexation of 4 at Different Temperatures with Variable Amounts of 6 in Acetone-d_6 As Determined by the Rose−Drago Method

			K (M^{-1})			
proton	T (°C)	count[a]	mean	std dev	CI 95%[b]	median
H_a	21.8	21	234	55	23	232
H_a	30.0	21	182	122	52	153
H_a	38.0	21	100	44	19	91
H_a	46.0	21	63.1	28.3	12	58.4
H_a	54.0	21	44.3	22.5	9.6	39.2
H_b	21.8	21	232	33	14	230
H_b	30.0	21	152	47	20	147
H_b	38.0	21	96.6	37.4	16.0	90.7
H_b	46.0	21	61.7	20.2	8.6	55.7
H_b	54.0	21	42.2	12.1	5.2	42.0

[a] Number of values of K obtained from individual line crossings in the plot of $1/K$ vs Δ_0. [b] Confidence interval about the mean at the 95% probability level.

Table 7. Comparison of Initial and Final Association Constants Determined for the Complexation of 4 with 6 by Benesi−Hildebrand and Scatchard Methods

		Benesi−Hildebrand		Scatchard	
temp (°C)	proton	K, initial (M^{-1})	K, final (M^{-1})	K, initial (M^{-1})	K, final (M^{-1})
21.8	H_a	135	253 ± 18	137	247 ± 25
21.8	H_b	138	259 ± 17	140	254 ± 22
30.0	H_a	101	178 ± 26	99.8	165 ± 33
30.0	H_b	98.1	170 ± 19	97.8	161 ± 26
38.0	H_a	65.7	104 ± 15	63.8	94.5 ± 19.1
38.0	H_b	65.6	103 ± 13	64.1	95.0 ± 17.4
46.0	H_a	45.7	66.0 ± 7.2	44.6	61.0 ± 9.7
46.0	H_b	46.1	66.7 ± 6.7	44.8	61.4 ± 9.5
54.0	H_a	33.7	45.6 ± 5.2	32.0	41.1 ± 7.6
54.0	H_b	34.9	47.6 ± 5.8	32.6	42.0 ± 8.1

the equation $(\Delta - \Delta_o)K = \Delta_o\Delta/(\Delta_o[\mathbf{4}]_o - \Delta[\mathbf{6}]_o)$. The intersections of the various pairs of lines are then used to estimate K. Results are given in Table 6.

Analyses of the data for protons H_a and H_b gave the same K values at a given temperature within the error limits (Tables 3−6). The importance of using such iterative techniques is indicated in Table 7. It can be seen that use of the simple forms of the Benesi-Hildebrand and Scatchard methods in which $[\mathbf{6}]_o$, the total initial concentration of **6**, is used to estimate $[\mathbf{6}]$, results in underestimation of the association constants, in these cases by a factor of up to 2.[18] Since the difference between $[\mathbf{6}]$ and $[\mathbf{6}]_o$ increases with K, the disparity between the simple and iterative treatments is ampified for systems with higher association constants. As demonstrated in Table 8 the K values derived from all four methods agree well with one another, as do the free energies of complexation, ΔG (Table 9).

With K values in hand, the fraction of **4** existing as pseudorotaxane **7** was calculated (Table 10 and Figure 4). Since ΔG is more negative and K is higher at lower temperature (Tables 8 and 9), the fraction of pseudorotaxane **7** increased with decreasing temperature at a given concentration. On the other hand, at a given temperature, the conversion to **7** increased as more paraquat **6** was added, in accord with the equilibrium process.

The van't Hoff plots (Table 11) afforded more valuable information, ΔH (−44.7 kJ/mol) and ΔS (−106 J/mol deg). The negative enthalpy agrees with strong attractive interactions, π-stacking accompanied by H-bonding, and dipolar−dipolar interactions, between the crown ether and the paraquat moieties. The negative entropy is obvious because pseudorotaxane **7** is more organized and rigid than the individual starting materials **4** and **6**.

Thus proton NMR spectroscopy can be effectively used for quantitative characterization of these supermolecular systems. Considering that no ΔH and ΔS values appear to have been reported for complexation between crown ethers and paraquat derivatives, despite the fact that the complexation has widely been used to construct

Table 8. Comparison of Association Constants for the Complexation of 4 with 6 in Acetone-d_6 at Different Temperatures As Determined by Various Plotting Methods

		K, final (M^{-1})		K (M^{-1})		
temp (°C)	proton	Benesi−Hildebrand	Scatchard	Creswell−Allred	Rose−Drago	av $K_{a,b}$ (M^{-1})
21.8	H_a	253 ± 18	246 ± 25	244 ± 55	234 ± 23	247 ± 26
	H_b	259 ± 17	254 ± 22	251 ± 38	232 ± 14	
30.0	H_a	178 ± 26	165 ± 33	162 ± 45	182 ± 52	166 ± 32
	H_b	170 ± 19	161 ± 26	158 ± 38	152 ± 20	
38.0	H_a	104 ± 15	94.5 ± 19.1	91.9 ± 11.2	100 ± 19	97.2 ± 15.1
	H_b	103 ± 13	95.0 ± 17.4	92.2 ± 10.4	96.6 ± 16.0	
46.0	H_a	66.0 ± 7.2	61.0 ± 9.7	59.4 ± 3.9	63.1 ± 12.1	62.3 ± 7.8
	H_b	66.7 ± 6.7	61.4 ± 9.5	59.3 ± 4.3	61.7 ± 8.6	
54.0	H_a	45.6 ± 5.2	41.1 ± 7.6	39.5 ± 2.9	44.3 ± 9.6	42.8 ± 5.9
	H_b	47.6 ± 5.8	42.0 ± 8.1	39.9 ± 3.1	42.2 ± 5.2	

Table 9. Change in Gibbs Free Energy for the Complexation of 4 with 6 in Acetone-d_6 at Different Temperatures As Determined by Various Plotting Methods[a]

		ΔG (kJ/mol)				
temp (°C)	proton	Benesi−Hildebrand	Scatchard	Creswell−Allred	Rose−Drago	av $\Delta G_{a,b}$ (kJ/mol)
21.8	H_a	−13.6 ± 0.2	−13.5 ± 0.2	−13.5 ± 0.5	−13.4 ± 0.2	13.5 ± 0.2
	H_b	−13.6 ± 0.2	−13.6 ± 0.2	−13.5 ± 0.3	−13.4 ± 0.1	
30.0	H_a	−13.1 ± 0.3	−12.9 ± 0.5	−12.8 ± 0.6	−13.1 ± 0.6	12.9 ± 0.4
	H_b	−13.0 ± 0.3	−12.8 ± 0.4	−12.8 ± 0.5	−12.7 ± 0.3	
38.0	H_a	−12.0 ± 0.3	−11.8 ± 0.5	−11.7 ± 0.3	−11.9 ± 0.4	11.8 ± 0.4
	H_b	−12.0 ± 0.3	−11.8 ± 0.4	−11.7 ± 0.3	−11.8 ± 0.4	
46.0	H_a	−11.1 ± 0.3	−10.9 ± 0.4	−10.8 ± 0.2	−11.0 ± 0.5	10.9 ± 0.3
	H_b	−11.1 ± 0.3	−10.9 ± 0.4	−10.8 ± 0.2	−10.9 ± 0.3	
54.0	H_a	−10.4 ± 0.3	−10.1 ± 0.5	−10.0 ± 0.2	−10.3 ± 0.5	10.2 ± 0.4
	H_b	−10.5 ± 0.3	−10.2 ± 0.5	−10.0 ± 0.2	−10.2 ± 0.3	

[a] Error estimates are based on the error associated with corresponding values of K.

Table 10. Fractional Conversion to 7 under Different Conditions with $[4]_0 = 7.350$ mM

	[7]/[4]$_0$[a]				
[6]$_0$ (mM)	21.8 °C	30.0 °C	38.0 °C	46.0 °C	54.0 °C
11.63	0.640 ± 0.002	0.565 ± 0.005	0.457 ± 0.005	0.366 ± 0.005	0.296 ± 0.008
23.25	0.810 ± 0.002	0.739 ± 0.004	0.633 ± 0.007	0.543 ± 0.008	0.457 ± 0.011
27.44	0.831 ± 0.002	0.758 ± 0.005	0.657 ± 0.008	0.568 ± 0.008	0.488 ± 0.012
39.23	0.891 ± 0.002	0.850 ± 0.007	0.774 ± 0.009	0.682 ± 0.009	0.589 ± 0.014
44.18	0.903 ± 0.002	0.860 ± 0.005	0.790 ± 0.009	0.710 ± 0.010	0.632 ± 0.015
65.16	0.933 ± 0.002	0.899 ± 0.005	0.840 ± 0.010	0.776 ± 0.011	0.698 ± 0.017
122.4	0.981 ± 0.002	0.978 ± 0.006	0.946 ± 0.011	0.905 ± 0.013	0.870 ± 0.021

[a] Average of six values obtained from Benesi−Hildebrand, Scatchard, and Creswell−Allred methods using H_a and H_b. Error based on the confidence interval of the mean at the 95% probability level.

Table 11. ΔH and ΔS for the Complexation of 4 with 6 to Form 7 and 5 with 6 To Form 8 in Acetone-d_6 As Determined by Various Plotting Methods[a]

	4 + 6		5 + 6	
method	ΔH (kJ/mol)	ΔS (J/mol deg)	ΔH (kJ/mol)	ΔS (J/mol deg)
Benesi−Hildebrand	−43.6 ± 2.3	−102 ± 7	−23.2 ± 4.5	−45.1 ± 14.5
Scatchard	−45.6 ± 1.8	−108 ± 6	−26.8 ± 2.8	−57.4 ± 9.0
Creswell−Allred	−46.4 ± 1.8	−111 ± 6	−28.8 ± 2.3	−64.1 ± 7.4
Rose−Drago	−43.3 ± 3.7	−101 ± 12	−27.3 ± 3.0	−59.0 ± 9.7
av	−44.7 ± 2.4	−106 ± 8	−26.5 ± 3.2	−56.4 ± 10.2

[a] Error estimates are based on statistically determined confidence limits of the slope and intercept of van't Hoff plots at the 95% probability level. Association constants determined from the chemical shift changes of H_a and H_b, or of H_A and H_B plotted together.

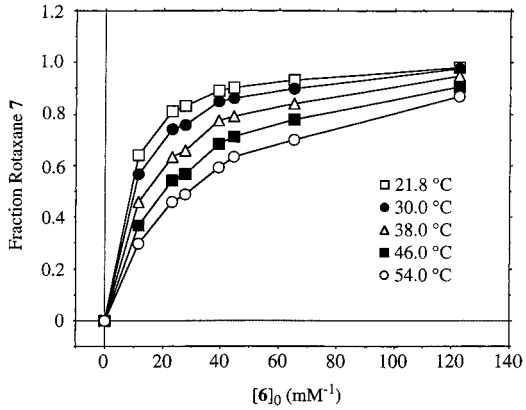

Figure 4. Dependence of the fraction of [2]pseudorotaxane **7** ([**7**]/[**4**]$_o$) vs the feed concentration of **6** with [**4**]$_o$ = 7.350 mM in acetone at different temperatures.

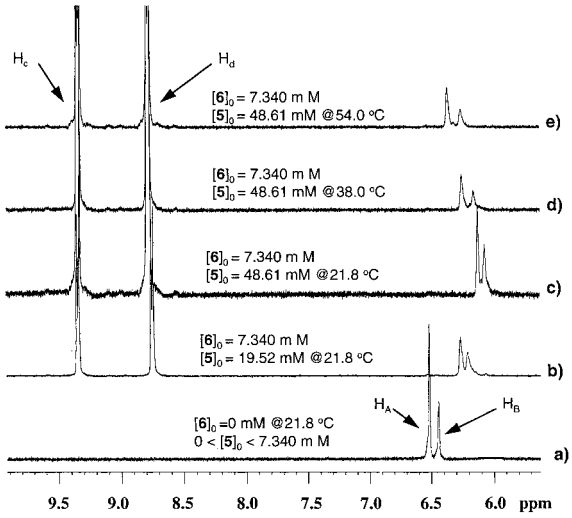

Figure 5. Expanded aromatic regions of the 400 MHz proton NMR spectra for (a) **5** and (b−e) solutions of **5** and **6** in acetone-d_6.

supermolecules,[1,7,10,11] the present results constitute the basis for improved quantitative understanding of these systems.

(b) Polypseudorotaxane 8. The model complexation study proved that the diester-functionalized 32-membered crown ether **4** effectively complexes with paraquat **6**. Therefore, the analogous poly(ester crown ether) **5** is expected to complex with paraquat **6** to produce designed polyrotaxane **8** (Scheme 2).

Not surprisingly, as soon as **6** was added to a solution of **5** in acetone, an orange color immediately appeared, indicating the rapid formation of polypseudorotaxane **8**. Again, direct evidence was obtained from proton NMR studies. Compared to those of pure **5** (Figure 5a), the signals of the aromatic protons H_A and H_B (see Scheme 2) of the macrocyclic moiety in polypseudorotaxane **8** (Figure 5b,c) shifted upfield; this is consistent with polypseudorotaxane formation, i.e., the existence of through space interactions because of π-stacking between these two components.[1,7,10,11] Increasing temperature disfavors the formation of **8** as manifested by the fact that the signals of protons H_A ands H_B shifted downfield (Figure 5c−e) at higher temperature. All these signals are time-averaged, since no separate peaks corresponding to threaded and unthreaded structures exist in the spectra. Therefore, although the cyclic host component was incorporated into the polymeric backbone, the exchange process is rapid relative to the proton NMR time scale.

As with the model system, to analyze the equilibrium quantitatively, it was necessary to measure the chemical shifts of protons H_A and H_B at different solution compositions (**5** + **6**) and temperatures (Table 12). The corresponding Δ values were calculated relative to those of pure **5** (Table 13).

The same four methodologies were used to analyze these data; the results (K and Δ_o values) are shown in Tables 14−17. First and seventh generation Benesi−Hildebrand plots are shown in Figure 3. As with the model system, results using data based on H_A and H_B are indistinguishable within experimental error as shown in Table 18. ΔG values are given in Table 19. There is good agreement among the four methods.

From the van't Hoff plots based on these K values, ΔH and ΔS were derived to be −26.5 kJ/mol and −56.4

Table 12. Chemical Shifts of Protons H_A and H_B of 5 upon Complexation with Different Amounts of 6 in Acetone at Different Temperatures[a]

	δ_A/δ_B[b] (ppm)				
$[6]_o$ (mM)	21.8 °C	30.0 °C	38.0 °C	46.0 °C	54.0 °C
0	6.517/6.441	6.521/6.447	6.520/6.453	6.521/6.459	6.527/6.466
11.16	6.330/6.271	6.375/6.307	6.413/6.339	6.441/6.364	6.465/6.391
19.52	6.265/6.206	6.316/6.242	6.366/6.287	6.404/6.320	6.439/6.356
32.54	6.179/6.119	6.248/6.172	6.304/6.215	6.355/6.260	6.398/6.306
37.43	6.167/6.111	6.224/6.150	6.289/6.196	6.343/6.245	6.390/6.291
42.55	6.149/6.094	6.213/6.137	6.272/6.183	6.329/6.229	6.377/6.278
48.61	6.126/6.070	6.194/6.117	6.250/6.160	6.315/6.211	6.364/6.255
67.00	6.095/6.042	6.156/6.079	6.218/6.121	6.275/6.166	6.330/6.217
100.8	6.062/6.010	6.118/6.040	6.179/6.078	6.237/6.117	6.294/6.167

[a] $[5]_o$ constant at 7.340 mM; temp, ±0.1 °C. [b] δ_A/δ_B: the chemical shifts of the protons H_A and H_B, respectively (±0.001 ppm).

Table 13. Chemical Shift Changes of Protons H_A and H_B of 5 (7.340 mM Initially) upon Complexation with Different Amounts of 6 in Acetone at Different Temperatures

	Δ_A/Δ_B (ppm)[a]				
$[6]_o$ (mM)	21.8 °C	30.0 °C	38.0 °C	46.0 °C	54.0 °C
0	0/0	0/0	0/0	0/0	0/0
11.16	0.187/0.170	0.146/0.140	0.107/0.114	0.080/0.095	0.062/0.075
19.52	0.252/0.235	0.205/0.205	0.154/0.166	0.117/0.139	0.088/0.110
32.54	0.338/0.322	0.273/0.275	0.216/0.238	0.166/0.199	0.129/0.165
37.43	0.350/0.330	0.297/0.297	0.231/0.257	0.178/0.214	0.137/0.175
42.55	0.368/0.347	0.308/0.310	0.248/0.270	0.192/0.230	0.150/0.188
48.61	0.391/0.371	0.327/0.330	0.270/0.293	0.206/0.248	0.163/0.211
67.00	0.422/0.399	0.365/0.368	0.302/0.332	0.246/0.293	0.197/0.249
100.8	0.455/0.431	0.403/0.407	0.341/0.375	0.284/0.342	0.233/0.299

[a] Δ_A/Δ_B: the chemical shifts changes of protons H_A and H_B compared to those of pure **5** at the corresponding temperatures, respectively (±0.002 ppm).

Table 14. Association Constants for the Complexation of 5 at Different Temperatures with Variable Amounts of 6 in Acetone-d_6 As Determined by Iterative Benesi−Hildebrand Plotting Techniques[a]

					Δ_0 (ppm)		
T (°C)	proton	slope (mM·ppm)	intercept (ppm^{-1})	R^2	entered	calcd	K[b] (M^{-1})
21.8	H_A	30.0764	1.9068	0.994	0.52444	0.52444	63.4 ± 6.3
21.8	H_B	34.9084	1.94189	0.996	0.51496	0.51496	55.6 ± 4.7
30.0	H_A	43.3368	2.08001	0.997	0.48077	0.48077	48.0 ± 3.7
30.0	H_B	47.6314	1.95778	1.000	0.51078	0.51078	41.1 ± 1.0
38.0	H_A	67.4799	2.27168	0.997	0.44020	0.44020	33.7 ± 3.2
38.0	H_B	64.7974	2.01456	0.998	0.49639	0.49639	31.1 ± 2.7
46.0	H_A	95.7814	2.68877	0.997	0.37192	0.37192	28.1 ± 3.1
46.0	H_B	81.5280	2.20799	0.997	0.4529	0.4529	27.1 ± 3.0
54.0	H_A	127.729	3.31271	0.991	0.30187	0.30187	25.9 ± 5.1
54.0	H_B	110.231	2.38273	0.995	0.41969	0.41969	21.6 ± 3.5

[a] Δ_0 and K were obtained from the seventh generation Benesi−Hildebrand plot. [b] Error estimates are based on statistically determined confidence limits of the intercept and slope at the 95% probability level propagated according to

$$\Delta K = K\sqrt{\left(\frac{\Delta\text{intercept}}{\text{intercept}}\right)^2 + \left(\frac{\Delta\text{slope}}{\text{slope}}\right)^2}$$

J/mol deg, respectively (Table 11). Therefore, the formation of polypseudorotaxane **8** is favored by the enthalpy term but disfavored by the entropy term.

Compared to the model system **4** + **6** ⇌ **7** (Table 8), the equilibium constants for the polymeric system **5** + **6** ⇌ **8** (Table 18) are lower. The difference, we believe, results from the reduced flexibility of the cyclic units of polyester **5** relative to those of diester **4**. For pseudorotaxane formation and π-stacking to occur,[10a] the phenylene rings of the cyclic have to rotate toward each other relative to their parallel but nonoverlapped conformation in the uncomplexed state.[19] As soon as they are incorporated into the polymer backbone of **5**, the rotation of these phenylene rings becomes much more difficult because it involves local, or probably more extensive, chain movement; this leads to an enthalpic penalty. Thus, ΔH is more negative for the model system. However, since the conformations of the cyclic moiety in polymer **5** are already restricted and less flexible relative to free macrocycle **4**, while both of them will be rigidified upon complexation with **6**, ΔS for the model system is more negative than for the polymeric system. Thus, while on a relative basis the enthalpic term is more favorable for [2]pseudorotaxane **7**, the entropic term is less disfavorable for polypseudorotaxane **8**.

With the knowledge gained from these studies the m/n value, the mole fraction of complexed macrocyclic units, ($=\Delta/\Delta_o$), of polyrotaxane **8** can be simply controlled by varying temperature and/or concentration. m/n increases with increasing ratio of paraquat **6** vs poly(crown ether) **5** at a given temperature, as well as with decreasing temperature at given concentrations (Table 20 and Figure 6).

III. Physical Properties of Polypseudorotaxanes 8. (a) Solubility. To understand the effect of

Table 15. Association Constants for the Complexation of 5 at Different Temperatures with Variable Amounts of 6 in Acetone-d_6 As Determined by Iterative Scatchard Plotting Techniques[a]

					Δ_0 (ppm)		
T (°C)	proton	slope (mM^{-1})	intercept ($ppm \cdot mM^{-1}$)	R^2	entered	calcd	K^b (M^{-1})
21.8	H_A	−0.05999	0.032076	0.985	0.534697	0.534697	60.0 ± 7.3
21.8	H_B	−0.05422	0.028192	0.987	0.519996	0.519996	54.2 ± 6.3
30.0	H_A	−0.04521	0.022265	0.991	0.492523	0.492523	45.2 ± 4.3
30.0	H_B	−0.04064	0.020861	0.999	0.513256	0.513256	40.6 ± 1.4
38.0	H_A	−0.03153	0.014322	0.988	0.454286	0.454286	31.5 ± 3.4
38.0	H_B	−0.03018	0.015204	0.988	0.503843	0.503843	30.2 ± 3.3
46.0	H_A	−0.02482	0.009844	0.980	0.396583	0.396583	24.8 ± 3.5
46.0	H_B	−0.02415	0.011621	0.983	0.481230	0.481230	24.2 ± 3.1
54.0	H_A	−0.02090	0.007105	0.949	0.339977	0.339977	20.9 ± 4.8
54.0	H_B	−0.01861	0.008522	0.969	0.458008	0.458008	18.6 ± 3.3

[a] Δ_0 and K were obtained from the seventh generation Scatchard plot. [b] Error estimates are based on statistically determined confidence limits of the slope at the 95% probability level.

Table 16. Association Constants for the Complexation of 5 at Different Temperatures with Variable Amounts of 6 in Acetone-d_6 As Determined by Iterative Creswell−Allred Plotting Techniques

T (°C)	proton	|slope| = Δ_0 (ppm)	intercept (ppm)	R^2	$\delta_{intercept}/\delta_{free}$[a]	K^b (M^{-1})
21.8	H_A	0.5372	6.517	0.997	0.99999996	59.0 ± 1.7
21.8	H_B	0.5186	6.441	0.996	1.0000006	54.6 ± 1.8
30.0	H_A	0.4972	6.521	0.999	1.00000004	44.0 ± 0.9
30.0	H_B	0.5137	6.447	1	1.0000009	40.5 ± 0.4
38.0	H_A	0.4578	6.52	0.999	1.00000007	30.9 ± 0.7
38.0	H_B	0.5118	6.453	0.999	1.00000000	29.4 ± 0.5
46.0	H_A	0.4073	6.521	0.998	1.00000000	23.4 ± 0.6
46.0	H_B	0.4934	6.459	0.999	0.99999999	22.9 ± 0.5
54.0	H_A	0.3554	6.527	0.997	0.99999991	19.1 ± 0.7
54.0	H_B	0.476	6.466	0.998	1.00000001	17.2 ± 0.5

[a] The number of digits displayed is not meant to suggest degree of significance, but rather to illustrate the degree of convergence used to obtain K. [b] Δ_0 determined from the slope was used to calculate K at each temperature according to the expression

$$K = \frac{1}{\left(\frac{\Delta_0}{\Delta} - 1\right)[S_0] - \left(1 - \frac{\Delta}{\Delta_0}\right)[R_0]}$$

The confidence interval about the mean at the 95% probability level is used here to express the uncertainty in K.

Table 17. Association Constants for the Complexation of 5 at Different Temperatures with Variable Amounts of 6 in Acetone-d_6 As Determined by the Rose−Drago Method

			K (M^{-1})			
proton	T (°C)	count[a]	mean	std dev	CI 95%[b]	median
H_A	21.8	28	59.4	17.4	6.4	58.4
H_A	30.0	28	43.4	9.8	3.6	40.8
H_A	38.0	28	30.1	7.3	2.7	29.6
H_A	46.0	28	24.5	6.1	2.3	23.4
H_A	54.0	28	21.1	9.7	3.6	17.7
H_B	21.8	28	58.0	24.7	9.1	54.0
H_B	30.0	28	39.9	5.2	1.9	39.9
H_B	38.0	28	29.6	6.4	2.4	29.1
H_B	46.0	28	23.9	5.2	1.9	22.2
H_B	54.0	28	18.4	6.8	2.5	17.2

[a] Number of values of K obtained from individual line crossings in the plot of $1/K$ vs Δ_0. [b] Confidence interval about the mean at the 95% probability level.

m/n on the solubility of polypseudorotaxane **8**, samples were prepared by slowly cooling acetone solutions of **5** and **6** to −78 °C, followed by freeze-drying. The orange color of the resultant solids indicated that the polypseudorotaxane structure **8** was retained in the solid state. On the basis of the measured ΔH and ΔS values, K is estimated to be 2.29×10^4 M^{-1} at −78 °C. Therefore, under such conditions the solids obtained had m/n values essentially equal to the feed ratios (≤1) (Table 21), i.e., pseudorotaxane formation was nearly quantitative.

Since paraquat **6** and starting polymer **5** had different solubilities, the solubility of polypseudorotaxane **8** depended on the m/n value. Not surprisingly, all the freeze-dried polyspeudorotaxanes were soluble in DMF (Table 21), since it is a good solvent for both components. While polymer **5** is only slightly soluble in acetone, which is a good solvent for paraquat **6**, all the freeze-dried polypseudorotaxanes were soluble with an orange color. The lack of precipitation over several days at room temperature indicated that an m/n value of 0.248 (or less) is necessary to retain polymer **5** in the solution.

In THF polymer **5** is quite soluble, while paraquat **6** is not soluble. Interestingly, the freeze-dried polypseudorotaxanes **8** were initially soluble except for a small amount of uncomplexed paraquat even up to m/n = 0.997 (Table 21). However, after a few seconds, some paraquat **6** precipitated as a white solid as a result of dissociation of **8**. Since all the solutions remained orange and the precipitation stopped shortly after dissolution, the solubility of paraquat **6** was indeed enhanced by its complexation with polymer **5**.

In contrast, CH_3CN is a good solvent for paraquat **6**, but a nonsolvent for polymer **5**. However, all freeze-dried polypseudorotaxanes **8** with $m/n \geq 0.494$ were soluble in CH_3CN, while **8** with $m/n = 0.232$ was not (Table 21); this means that a certain m/n value is necessary for freeze-dried polypseudorotaxane **8** to be soluble. Interestingly, no insoluble materials were observed over weeks for freeze-dried **8** prepared with a feed ratio $[\mathbf{6}]_o/[\mathbf{5}]_o$ equal to 1 or greater; however, in solutions of freeze-dried **8** with m/n values lower than 0.75, precipitation of polymer **5** took place within a couple of minutes, indicating the occurrence of dethreading upon dissolution, presumably until **8** with m/n values greater than 0.734 resulted in solution.

(b) Viscosity. To study the effect of the formation of the polypseudorotaxane on chain conformation, the specific viscosity and reduced viscosity were measured in acetone at different feed ratios of **6** vs. **5** at a constant concentration of **5**. To eliminate the possible interference of the excess paraquat **6**, the viscosities were also calculated by subtracting the flow time contributed by **6**. As the results show, the incremental viscosity caused by **6** is negligible over the measured concentration range, i.e., η'_{sp}/C and η'_{sp} were very close to η_{sp}/C and η_{sp} (Table 22). Polypseudorotaxane **8** with $m/n = 0.517$ had a reduced viscosity (0.215 dL/g) and specific viscosity (0.122 dL/g) twice as high as those (0.122 and 0.0689 dL/g, respectively) of **8** with $m/n = 0.071$. Overall, the

Table 18. Comparison of Association Constants for the Complexation of 5 with 6 in Acetone-d_6 at Different Temperatures As Determined by Various Plotting Methods

		K, final (M^{-1})		K (M^{-1})		
temp (°C)	proton	Benesi−Hildebrand	Scatchard	Creswell−Allred	Rose−Drago	av $K_{A,B}$ (M^{-1})
21.8	H_A	63.4 ± 6.3	60.0 ± 7.3	59.0 ± 1.7	59.4 ± 6.4	58.0 ± 5.5
	H_B	55.6 ± 4.7	54.2 ± 6.3	54.6 ± 1.8	58.1 ± 9.1	
30.0	H_A	48.0 ± 3.7	45.2 ± 4.3	44.0 ± 0.9	43.4 ± 3.6	42.8 ± 2.2
	H_B	41.1 ± 1.0	40.6 ± 1.4	40.5 ± 0.4	39.9 ± 1.9	
38.0	H_A	33.7 ± 3.2	31.5 ± 3.4	30.9 ± 0.7	30.2 ± 2.7	30.8 ± 2.4
	H_B	31.1 ± 2.7	30.2 ± 3.3	29.4 ± 0.5	29.6 ± 2.4	
46.0	H_A	28.1 ± 3.1	24.8 ± 3.5	23.4 ± 0.6	24.5 ± 2.3	24.9 ± 2.3
	H_B	27.1 ± 3.0	24.2 ± 3.1	22.9 ± 0.5	23.9 ± 1.9	
54.0	H_A	25.9 ± 5.1	20.9 ± 4.8	19.1 ± 0.7	21.1 ± 3.6	20.4 ± 3.0
	H_B	21.6 ± 3.5	18.6 ± 3.3	17.2 ± 0.5	18.4 ± 2.5	

Table 19. Changes in Gibbs Free Energy for the Complexation of 5 with 6 To Form 8 in Acetone-d_6 at Different Temperatures As Determined by Various Plotting Methods[a]

		ΔG (kJ/mol)				
temp (°C)	proton	Benesi−Hildebrand	Scatchard	Creswell−Allred	Rose−Drago	av $\Delta G_{A,B}$ (kJ/mol)
21.8	H_A	−10.2 ± 0.2	−10.0 ± 0.3	−10.0 ± 0.1	−10.0 ± 0.3	10.0 ± 0.2
	H_B	−9.9 ± 0.2	−9.8 ± 0.3	−9.8 ± 0.1	−10.0 ± 0.4	
30.0	H_A	−9.8 ± 0.2	−9.6 ± 0.2	−9.5 ± 0.1	−9.5 ± 0.2	9.5 ± 0.2
	H_B	−9.4 ± 0.1	−9.3 ± 0.1	−9.3 ± 0.1	−9.3 ± 0.1	
38.0	H_A	−9.1 ± 0.2	−8.9 ± 0.3	−8.9 ± 0.1	−8.8 ± 0.2	8.9 ± 0.2
	H_B	−8.9 ± 0.2	−8.8 ± 0.3	−8.7 ± 0.1	−8.8 ± 0.2	
46.0	H_A	−8.8 ± 0.3	−8.5 ± 0.4	−8.4 ± 0.1	−8.5 ± 0.2	8.5 ± 0.2
	H_B	−8.8 ± 0.3	−8.4 ± 0.3	−8.3 ± 0.1	−8.4 ± 0.2	
54.0	H_A	−8.9 ± 0.5	−8.3 ± 0.6	−8.0 ± 0.1	−8.3 ± 0.4	8.2 ± 0.4
	H_B	−8.4 ± 0.4	−8.0 ± 0.4	−7.7 ± 0.1	−7.9 ± 0.4	

[a] Error estimates are based on the error associated with corresponding values of K.

Table 20. The m/n Values of 8 Formed under Different Conditions with $[5]_0 = 7.340$ mM

	m/n[a]				
$[6]_0$ (mM)	21.8 °C	30.0 °C	38.0 °C	46.0 °C	54.0 °C
11.16	0.340 ± 0.010	0.286 ± 0.011	0.232 ± 0.006	0.202 ± 0.007	0.177 ± 0.013
19.52	0.464 ± 0.009	0.409 ± 0.009	0.336 ± 0.007	0.296 ± 0.010	0.255 ± 0.017
32.54	0.629 ± 0.007	0.547 ± 0.010	0.476 ± 0.007	0.421 ± 0.014	0.378 ± 0.023
37.43	0.648 ± 0.010	0.593 ± 0.013	0.511 ± 0.007	0.453 ± 0.015	0.401 ± 0.025
42.55	0.681 ± 0.011	0.617 ± 0.012	0.543 ± 0.010	0.487 ± 0.016	0.436 ± 0.029
48.61	0.726 ± 0.01	0.656 ± 0.012	0.59 ± 0.011	0.524 ± 0.017	0.481 ± 0.028
67.00	0.782 ± 0.011	0.731 ± 0.014	0.655 ± 0.016	0.623 ± 0.021	0.574 ± 0.037
100.8	0.844 ± 0.012	0.808 ± 0.014	0.750 ± 0.011	0.723 ± 0.024	0.684 ± 0.041

[a] Average of six values obtained from Benesi−Hildebrand, Scatchard, and Creswell−Allred methods using H_A and H_B. Error based on the confidence interval of the mean at the 95% probability level.

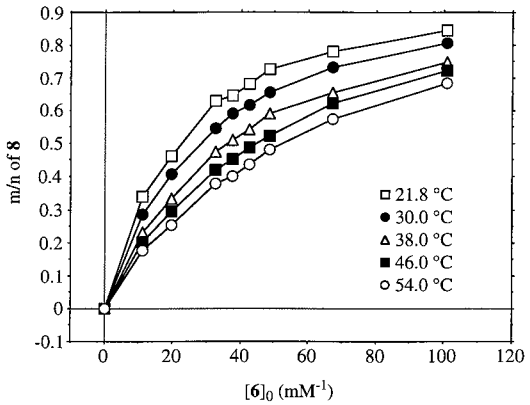

Figure 6. Dependence of the m/n value of **8** on the feed concentration of **6** with $[5]_o = 7.340$ mM in acetone at different temperatures.

Table 21. Solubilities of 5, 6, and 8[a]

	$[5]_0$[b] (mM)	$[6]_0$[b] (mM)	m/n[c]	acetone	THF	CH_3CN	DMF
6	0	7.60		Y	N	Y	Y
5	<7.60[d]	0	0	P	Y	N	Y
8	7.60	1.90	0.248	$Y^{5,6}$	Y^5,P^6	N	$Y^{5,6}$
8	7.60	3.80	0.494	$Y^{5,6}$	Y^5,P^6	$[Y^{5,6}/N^5,Y^6]$[e]	$Y^{5,6}$
8	7.60	5.70	0.734	$Y^{5,6}$	Y^5,P^6	$[Y^{5,6}/N^5,Y^6]$[e]	$Y^{5,6}$
8	7.60	7.60	0.927	$Y^{5,6}$	Y^5,P^6	$Y^{5,6}$	$Y^{5,6}$
8	7.60	15.2	0.994	$Y^{5,6}$	Y^5,P^6	$Y^{5,6}$	$Y^{5,6}$
8	7.60	22.8	0.997	$Y^{5,6}$	Y^5,P^6	$Y^{5,6}$	$Y^{5,6}$

[a] Y^x: component ***x*** totally soluble; P^x: ***x*** component partially soluble; insoluble part and precipitate were identified by solubility in CH_3CN and THF and confirmed by ^1H NMR; N^x: ***x*** component insoluble. [b] The initial concentrations of **5** and **6**. [c] The m/n values of solid **8** from freeze-drying calculated based on $K = 2.29 \times 10^4$ M^{-1} at −78 °C. [d] Polymer **5** by itself only partially soluble in acetone. [e] Initially both components were soluble but polymer **5** precipitated in less than 10 seconds.

higher the m/n, the higher the viscosity of polypseudorotaxane **8** (Figure 7); this clearly indicates that **8** with higher m/n had larger hydrodynamic volume. Several factors could be involved. Of course, the solvated volume of the polymer will increase as more paraquat guests are taken in. Moreover, the presence of the dicationic paraquat guest species within the cavities of the host macrocyclic units of the polymer backbone would be expected to rigidify the macrocycle and cause chain extension through a polyelectrolyte effect, i.e., ionic repulsion. Additionally, as m/n increases the solubility parameter for the polymer changes,

Table 22. Viscosities[a] and Glass Transition Temperatures of 8 with Different *m*/*n* Values

	$[\mathbf{5}]_0$[b] (mM)	$[\mathbf{6}]_0$[b] (mM)	*m*/*n*[c]	η'_{sp}[d]	η'_{sp}/C[d] (dL/g)	η_{sp}[d]	η_{sp}/C[d] (dL/g)	*m*/*n*[e]	T_g[f] (°C)
5			0					0	−6.3
8	7.427	1.857	0.071	0.0682	0.120	0.0689	0.122		
8	7.427	3.714	0.136	0.0761	0.134	0.0770	0.136	0.494	44.6
8	7.427	5.570	0.193	0.0830	0.147	0.0841	0.148	0.734	85.6
8	7.427	7.427	0.245	0.0928	0.164	0.0942	0.166	0.926	115.5
8	7.427	14.85	0.407	0.107	0.189	0.110	0.194		
8	7.427	22.28	0.517	0.118	0.208	0.122	0.215		

[a] Measured with Cannon L12 viscometer in acetone at 21.8 °C at the concentrations specified. [b] The feed concentration of polymer **5** (repeat unit basis) and **6**, respectively; 7.427 mM of **5** equals 0.5667 g/dL. [c] Calculated based on $K = 58.0\ M^{-1}$ in acetone at 21.8 °C. [d] $\eta'_{sp} = (t - t_o')/t_o'$ and $\eta'_{sp}/C = (t - t_o')/t_o'C$ where t and t_o' are the flow times of the solution of **5** and **6** and solution of pure **6** (the concentrations of **6** were same for both solutions) in acetone at 21.8 °C, respectively, and C is the concentration of **5**. $\eta_{sp} = (t - t_o'')/t_o$ and $\eta_{sp}/C = (t - t_o')/t_oC$ (t_o = flow time of acetone). [e] Calculated based on $K = 2.29 \times 10^4\ M^{-1}$ because the samples for T_g were obtained by freeze-drying at −78 °C. [f] Measured by DSC at scan rate of 10 °C/min.

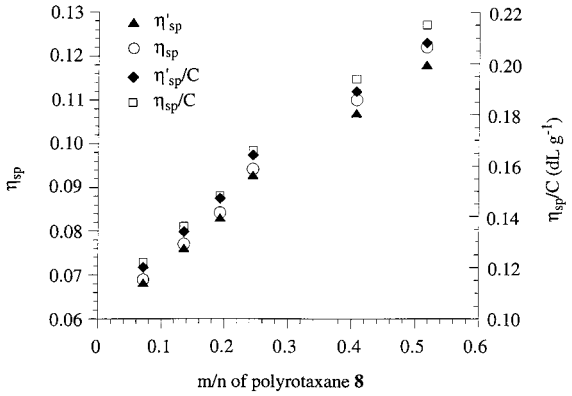

Figure 7. Dependence of the viscosity of **8** on the *m*/*n* value in acetone at 21.8 °C.

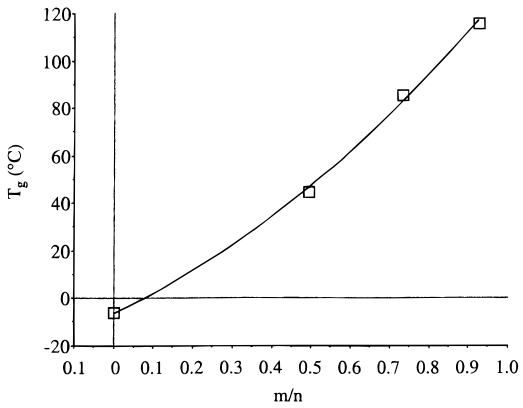

Figure 8. Dependence of the glass transition (T_g) of freeze-dried samples of **8** on the *m*/*n* value.

and hence its interactions with the solvent change; polyester **5** is only slightly soluble in acetone (Table 21), and hence at low *m*/*n* values polymer **8** will not be well solvated, but as *m*/*n* increases the "goodness" of the solvent will increase and the polymer will assume more extended conformations.

(c) Glass Transition Temperatures and Melt Dethreading. The samples from the viscosity measurements were freeze-dried in an acetone/dry ice bath (−78 °C) under high vacuum for thermal analysis. According to K ($2.29 \times 10^4\ M^{-1}$) calculated from ΔH and ΔS at this temperature, *m*/*n* values of the resulting **8** were close to the feed ratios $[\mathbf{6}]_o/[\mathbf{5}]_o$ (≤ 1) (Table 22). Their deep orange color indicated that the pseudorotaxane structures persisted in the solid state. In the other words, solid polypseudorotaxanes can be prepared by simply mixing the two components in a common solvent, followed by freeze-drying. The corresponding physical properties and applications can then be explored.

While polymer **5** was a colorless, viscous material with a glass transition temperature (T_g) of −6.3 °C,[20] freeze-dried **8** (*m*/*n* = 0.734) was a glassy orange material with T_g = 85.6 °C, indicating that **8** is significantly more rigid. Overall, T_g increased with increasing *m*/*n* (Table 22, Figure 8), agreeing with expectation. The cyclic moiety contains flexible ethyleneoxy units; this explains the relatively low T_g of polyester **5**. Upon complexation with paraquat, this flexibility (the mobility of the cyclic) is restricted and the resultant polypseudorotaxane **8** is more rigid.

The freeze-dried polypseudorotaxanes upon heating above the glass transition temperatures lost their color, indicating that dethreading occurred. Slow cooling and reheating did not bring the color back; instead a glass transition temperature corresponding to pure polymer **5** was observed. Therefore, the dethreading is not reversible under these conditions, probably because paraquat **6,** which has a high melting point,[11] quickly phase separates upon dissociation. The color change upon heating introduces possible applications for these materials as ceiling temperature indicators, e.g., for storage and shipping of perishables; the switching temperature can be adjusted simply by means of the *m*/*n* value, which controls T_g.

Conclusions

An approach for new main chain polypseudorotaxanes of type **2** (Scheme 1) was described. Polypseudorotaxane **8** was effectively formed by threading linear paraquat **6** through the cavities of the cyclic repeat units of polymacrocycle **5**. The formation of the polypseudorotaxane structure in solution was indicated by the color change and quantified by proton NMR spectroscopy. The *m*/*n* value of polypseudorotaxane **8** increased with increasing amounts of paraquat **6**, as well as with decreasing temperature. The values of K, ΔH, and ΔS provide the basis for predicting the *m*/*n* values for the preparation of analogous systems. In both the model (**4** + **6** ⇌ **7**) and polymeric systems (**5** + **6** ⇌ **8**) pseudorotaxane formation is enthalpically driven. While entropic penalties are reduced in the polymer system relative to the monomer system, enthalpic gains are likewise reduced, resulting in a lower association constant for the polymeric system.

Polypseudorotaxanes **8** with higher *m*/*n* values had higher solution viscosities. Importantly, solid-state polypseudorotaxanes with controlled *m*/*n* values were prepared by a simple freeze-drying procedure. The increased rigidity of **8** relative to starting polymer **5**

resulted in higher T_g's that increased with m/n. The solubility was also altered by the formation of polypseudorotaxane **8**, again depending on the m/n value.

The interaction of polymacrocycle **5** with a polyurethane containing backbone paraquat units derived from paraquat diol **6** resulted in the *reversible* formation of branched, interpenetrating network polypseudorotaxanes, as reported elsewhere.[21] Since paraquat **6** has two terminal −OH groups, polypseudorotaxane **8** can further react to form very interesting structures, e.g., polyrotaxane networks with diisocyanates. We are currently exploring such possibilities.

Experimental Section

Chemical Reagents and Measurements. All chemicals were reagent grade and used directly as received from Aldrich unless otherwise specified. All solvents were HPLC or GC grade. Bis(5-hydroxymethyl-1,3-phenylene)-32-crown-10 (**3**),[12] bis(5-acetoxymethyl-1,3-phenylene)-32-crown-10 (**4**),[12] and paraquat diol **6**[11] were prepared by well-established procedures. Proton NMR spectra, reported in ppm relative to tetramethylsilane (TMS), were obtained on a 400 MHz Varian spectrometer using acetone-d_6 or DMSO-d_6. The relative molecular weights of the polymer were measured by a GPC equipped with a UV detector using PS standards. T_g's were measured with a Perkin-Elmer thermal analysis system at a rate of 10 °C/minute; all reported values were the centers of transitions from the first heating.

Poly(ester crown ether) 5. Sebacoyl chloride (freshly distilled, 150.0 mg, 0.6272 mmol) and bis(5-hydroxymethyl-1,3-phenylene)-32-crown-10 (**3**) (374.3 mg, 0.6272 mmol) were dissolved in a mixture of anhydrous diglyme and DMSO (4 mL, 1:1 by volume). Polymerization proceeded at 60 °C for 2 days under the protection of N_2. The product was purified by precipitation into MeOH (100 mL) (421.1 mg, 88%). ^{1}H NMR (DMSO-d_6 ppm) δ 6.52 (br s, Ar*H*, 4H), 6.44 (br s, Ar*H*, 2H), 5.01 (br s, ArCH_2O, 4H), 4.06 (br s, ArCH_2CH$_2$O, 8H), 3.78 (br s, ArCH$_2$CH_2O, 8H), 3.61 (br s, ArCH$_2$CH$_2$OCH_2, 16H), 2.34 (br s, OOCH_2, 4H), 1.62 (br s, OOCH$_2$CH_2, 4H), 1.32 (br s, OOCH$_2$CH$_2$CH_2CH_2, 8H). M_n = 14.9 kg/mol and PDI = 1.97 by GPC with polystyrene standards.[22]

Acknowledgment. This work was supported by the National Science Foundation, Division of Materials Research, Grant No. DMR-97-06909.

References and Notes

(1) Reviews: (a) Gibson, H. W.; Bheda, M. C.; Engen, P. T. *Prog. Polym. Sci.* **1994**, *19*, 843. (b) Amabilino, D. B.; Stoddart, J. F. *Chem. Rev.* **1995**, *95*, 2725. (c) Philp, D.; Stoddart, J. F. *Angew. Chem., Int. Ed. Engl.* **1996**, *35*, 1154. (d) Gibson, H. W. In *Large Ring Molecules*; Semlyen, J. A., Ed.; J. Wiley and Sons: New York, 1996; pp 191−262. (e) Jäger, R.; Vögtle, F. *Angew. Chem., Int. Ed. Engl.* **1997**, *36*, 931. (f) Gong, C.; Gibson, H. W. *Curr. Opin. Solid State Mater. Sci.* **1998**, *2*, 647. (g) Nepolgodiev, S. A.; Stoddart, J. F. *Chem. Rev.* **1998**, *98*, XXXX.

(2) Main chain oligo- and polypseudorotaxanes and polyrotaxanes based on cyclodextrins as the cyclic component: Wenz, G. *Macromol. Symp.* **1994**, *87*, 11. Harada, A.; Li, J.; Kamachi, M. *Macromolecules* **1994**, *27*, 4538. Harada, A.; Okada, M.; Li, J.; Kamachi, M. *Macromolecules* **1995**, *28*, 8406. Weickenmeier, M.; Wenz, G. *Macromol. Rapid. Commun.* **1996**, *17*, 731. Steinbrunn, M. B.; Wenz, G. *Angew. Chem., Int. Ed. Engl.* **1996**, *35*, 2139. Yamaguchi, I.; Osakada, K.; Yamamoto, T. *J. Am. Chem. Soc.* **1996**, *118*, 1811. Herrmann, W.; Keller, B.; Wenz, G. *Macromolecules* **1997**, *30*, 4966. Herrmann, W.; Schneider, M.; Wenz, G. *Angew. Chem., Int. Ed. Engl.* **1997**, *36*, 2511. Ooya, T.; Yui, N. *J. Biomater. Sci., Polym. Ed.* **1997**, *8*, 437. Harada, A.; Li, J.; Kamachi, M. *J. Chem. Soc., Chem. Commun.* **1997**, 1413.

(3) Side chain polypseudorotaxanes and polyrotaxanes based on cyclodextrins as the cyclic component: Born, M.; Ritter, H. *Acta Polym.* **1994**, *45*, 68. Born, M.; Ritter, H. *Angew. Chem., Int. Ed. Engl.* **1995**, *34*, 309. Born, M.; Ritter, H. *Adv. Mater.* **1996**, *8*, 149. Born, M.; Ritter, H. *Macromol. Rapid Commun.* **1996**, *17*, 197. Noll, O.; Ritter, H. *Macromol. Rapid Commun.* **1997**, *18*, 53.

(4) Main chain polypseudorotaxanes and polyrotaxanes with ester repeat units based on crown ethers as the cyclic component: Gibson, H. W.; Liu, S.; Lecavalier, P.; Wu, C.; Shen, Y. X. *J. Am. Chem. Soc.* **1995**, *117*, 852. Gibson, H. W.; Liu, S.; Gong, C.; Ji, Q.; Joseph, E. *Macromolecules* **1997**, *30*, 3711. Gong, C.; Gibson, H. W. *Macromolecules* **1996**, *29*, 7029. Gong, C.; Gibson, H. W. *Macromol. Chem. Phys.* **1997**, *198*, 2331. Gong, C.; Ji, Q.; Glass, T. E.; Gibson, H. W. *Macromolecules* **1997**, *30*, 4807. Gong, C.; Gibson, H. W. *Macromolecules* **1997**, *30*, 8524.

(5) Main chain polypseudorotaxanes and polyrotaxanes with urethane repeat units based on crown ethers as the cyclic component: Shen, Y. X.; Xie, D.; Gibson, H. W. *J. Am. Chem. Soc.* **1994**, *116*, 537. Marand, E.; Hu, Q.; Gibson, H. W.; Veytsman, B. *Macromolecules* **1996**, *29*, 2555. Gong, C.; Gibson, H. W. *Angew. Chem., Int. Ed. Engl.* **1997**, *36*, 2331. Gong, C.; Gibson, H. W. *Macromolecules* **1998**, *31*, 308. Gong, C.; Subramanian, C.; Ji Q.; Gibson, H. W. *Macromolecules* **1998**, *31*, 1814.

(6) Polyrotaxanes by self-threading of functionalized crown ethers during polymerization: (a) Delaviz, Y.; Gibson, H. W. *Macromolecules* **1992**, *25*, 4859. (b) Gibson, H. W.; Nagvekar, D. S.; Powell, J.; Gong, C.; Bryant, W. S. *Tetrahedron* **1997**, *53*, 15197. (c) Gong, C.; Gibson, H. W. *J. Am. Chem. Soc.* **1997**, *119*, 8585. (d) Polyrotaxanes by self-threading of a functionalized crown ether during polymer modification: Gong, C.; Gibson, H. W. *J. Am. Chem. Soc.* **1997**, *119*, 5862.

(7) Main chain polypseudorotaxanes with paraquat repeat units based on crown ethers as the cyclic components: (a) Gibson, H. W.; Liu, S.; Shen, Y. X.; Bheda, M. C.; Lee, S.-H.; Wang, F. *NATO ASI Series*; Kluwer Acad. Pub., Dordrecht, The Netherlands, 1995; Series C, Vol. 456, pp 41−58. (b) Loveday, D.; Wilkes, G. L.; Bheda, M. C.; Shen, Y. X.; Gibson, H. W. *J. Macromol. Sci.—Pure Appl. Chem.* **1995**, *A32* (1), 1. (c) Schenning, A. P. H. J.; deBruin, B.; Rowan, A. E.; Kooijman, H.; Spek, A. L.; Nolte, R. J. M. *Angew. Chem., Int. Ed. Engl.* **1995**, *34*, 2132. Side chain polypseudorotaxanes with thiophene crown ether repeat units and paraquat derivatives as the guest species: (d) Marsella, M. J.; Carroll, P. J.; Swager, T. M. *J. Am. Chem. Soc.* **1995**, *117*, 9832. Main chain polypseudorotaxanes with arylene ether repeat units based on a bisparaquat macrocycle as the cyclic component: (e) Mason, P. E.; Parsons, I. W.; Tolley, M. S. *Angew. Chem., Int. Ed. Engl.* **1996**, *35*, 2238. (f) Owen, J. G.; Hodge, P. *J. Chem. Soc., Chem. Commun.* **1997**, 11. Main chain polypseudorotaxanes with methylenebis(aniline)-derived urethane repeat units based on a bisparaquat macrocycle as the cyclic component: (g) Mason, P. E.; Bryant, W. S.; Gibson H. W. *Macromolecules*, submitted for publication.

(8) Main chain polypseudorotaxanes with vinyl repeat units based on crown ethers as the cyclic components: Gibson, H. W.; Engen, P. T. *New. J. Chem.* **1993**, *17*, 723. Gibson, H. W.; Engen, P. T.; Lee, S.-H. *Polymer*, in press.

(9) Main chain polypseudorotaxanes with thiophene/2,2′-bipyridyl or thiophene/phenanthroline repeat units based on a phenanthroline-containing crown ether as the cyclic component via metal templating: Zhu, S. S.; Swager, T. M. *J. Am. Chem. Soc.* **1997**, *119*, 12568. Vidal, P. L.; Billon, M.; Divisia-Blohorn, B.; Bidan, G.; Kern, J.-M.; Sauvage, J.-P. *J. Chem. Soc., Chem. Commun.* **1998**, 1629. Main chain polyrotaxanes with pyrrole/2,2′-bipyridyl repeat units based on a phenanthroline-containing crown ether as the cyclic component via metal templating: Kern, J.-M.; Sauvage, J.-P.; Bidan, G.; Billon, M.; Divisia-Blohorn, B. *Adv. Mater.* **1996**, *8*, 580.

(10) (a) Allwood, B. L.; Spencer, N.; Shahriari-Zavareh, H.; Stoddart, J. F.; Williams, D. J. *J. Chem. Soc., Chem. Commun.* **1987**, 1058. (b) Gillard, R. E.; Raymo, F. M.; Stoddart, J. F. *Chem.—Eur. J.* **1997**, *3*, 1933.

(11) Shen, Y. X.; Engen, P. T.; Berg, M. A. G.; Merola, J. S.; Gibson, H. W. *Macromolecules* **1992**, *25*, 2786.

(12) Gibson, H. W.; Nagvekar, D. S. *Can. J. Chem.* **1997**, *75*, 1375.

(13) Tsukube, H.; Furuta, H.; Odani, A.; Takeda, Y.; Kudo, Y.; Inone, Y.; Liu, Y.; Sakamoto, H.; Kimura, K. *Comprehensive Supramolecular Chemistry*; Atwood, J. L., Davies, J. E. D., MacNicol, D. D., Vögtle, F., Eds.; Pergamon: Oxford, U.K., 1996; Vol. 6, pp 425−482.

(14) Benesi, H. A.; Hildebrand, J. H. *J. Am. Chem. Soc.* **1949**, *71*, 2703.

(15) Scatchard, G. *Ann. N. Y. Acad. Sci.* **1949**, *51*, 660.

(16) Cresswell, C. G.; Allred, A. L. *J. Phys. Chem.* **1962**, *66*, 1469.

(17) Rose, N. J.; Drago, R. S. *J. Am. Chem. Soc.* **1959**, *81*, 6138.
(18) Gong, C.; Gibson, H. W., *Angew Chem. Int. Ed. Engl.* **1998**, *37*, 310. The values for K, ΔH, and ΔS in this communication are incorrect, since they were based on the simple first-order Benesi−Hildebrand treatment of the data. The same data were employed in the present paper.
(19) The crystal structure of bis(*m*-phenylene)-32-crown-10 indicates an open cavity (4.9 × 7.8 Å), which undergoes a small conformational change when it complexes with paraquat.[10a] However, bis(5-carbomethoxy-1,3-phenylene)-32-crown-10 in the solid state has a collapsed cavity (0.75 × 7.8 Å), perhaps due to crystal packing forces and not intrinsic conformational preferences: Delaviz, Y.; Merola, J. S.; Berg M. A. G.; Gibson, H. W. *J. Org. Chem.* **1995**, *60*, 516.
(20) Polycondensation of **3** with sebacoyl chloride in the bulk state gave an elastomer with T_g = 2 °C via cross-linking with rotaxane units as a consequence of the self-association of **3**.[6b]
(21) Gong, C.; Gibson, H. W. *Macromolecular Chem. Phys.*, in press.
(22) DMSO as a competitive H-bonding cosolvent prevents self-association of **3** through H-bonding between its hydroxyl and ether groups; thus, no branching via self-threading to produce rotaxane units occurs.[6c] Therefore, polymer **5** was linear; the absence of rotaxane units in **5** was confirmed by the lack of signals for rings that cannot be threaded by **6** and therefore are not shifted in its presence in the ^{1}H NMR spectrum of **8** (Figure 5); see ref 6c for an example of the utilization of this effect to quantify the extent of self-threading.

MA971857S